J Comp Physiol B (1991) 161:635–646

Journal of Comparative Physiology B Biochemical, Systemic, and Environmental Physiology

Two-substrate kinetic analysis: a novel approach linking ion and acid-base transport at the gills of freshwater trout, *Oncorhynchus mykiss*

Greg G. Goss[1,*], and Chris M. Wood

Department of Biology, McMaster University, 1280 Main St. West, Hamilton, Ontario, Canada L8S 4K1

Accepted April 3, 1991

Summary. The novel application of a two-substrate model (Florini and Vestling 1957) from enzymology to transport kinetics at the gills of freshwater trout indicated that Na^+/acidic equivalent and Cl^-/basic equivalent flux rates are normally limited by the availability of the internal acidic and basic counterions, as well as by external Na^+ and Cl^- levels. Adult rainbow trout fitted with dorsal aortic and bladder catheters were chronically infused (10–16 h) with isosmotic HCl to induce a persistent metabolic acidosis. Acid-base neutral infusions of isosmotic NaCl and non-infused controls were also performed. Results were compared to previous data on metabolic alkalosis in trout induced by either isosmotic $NaHCO_3$ infusion or recovery from environmental hyperoxia (Goss and Wood 1990a, b). Metabolic acidosis resulted in a marked stimulation of Na^+ influx, no change in Cl^- influx, positive Na^+ balance, negative Cl^- balance, and net H^+ excretion at the gills. Metabolic alkalosis caused a marked inhibition of Na^+ influx and stimulation of Cl^- influx, negative Na^+ balance, positive Cl^- balance, and net H^+ uptake (=base excretion). Mean gill intracellular pH qualitatively followed extracellular pH. Classical one-substrate Michaelis-Menten analysis of kinetic data indicated that changes in Na^+ and Cl^- transport during acid-base disturbance are achieved by large increases and decreases in J_{max}, and by increases in K_m. However, one-substrate analysis considers only external substrate concentration and cannot account for transport limitations by the internal substrate. The kinetic data were fitted successfully to a two-substrate model, using extracellular acid-base data as a measure of internal HCO_3^- and H^+ availability. This analysis indicated that *true* J_{max} values for Na^+/acidic equivalent and Cl^-/basic equivalent transport are 4–5 times higher than *apparent* J_{max} values by one-substrate analysis. Flux rates are limited by the availability of the internal counterions; transport K_m values for HCO_3^- and H^+ are far above their normal internal concentrations. Therefore, small changes in acid-base status will have large effects on transport rates, and on apparent J_{max} values, without alterations in the number of transport sites. This system provides an automatic, negative feedback control for clearance or retention of acidic/basic equivalents when acid-base status is changing.

Key words: Gills – Ions – Acid-base – Kinetics – Intracellular pH – Trout, *Oncorhynchus mykiss*

Introduction

Acid-base homeostasis in fish is achieved largely by branchial fluxes of acidic and basic equivalents via carrier-mediated, electroneutral exchangers (Na^+/H^+, NH_4^+ and Cl^-/HCO_3^-, OH^-) and/or via electrogenic H^+ extrusion coupled to diffusive Na^+ entry through Na^+ channels located on the apical membranes of the gill epithelium [see McDonald and Prior (1988) and Avella and Bornancin (1989) for recent models]. Shaw (1959) was the first to show that uptake of Na^+ and Cl^- in freshwater animals showed characteristic first-order saturation kinetics as the external ion concentration ($[Na^+]_e$, $[Cl^-]_e$) was increased. These relationships could be described mathematically by the classic Michaelis-Menten analysis (designed for enzymes acting on one substrate) to yield estimates of the affinity ($1/K_m$) of the transport and the maximal rate of transport (J_{max}) for the external ion. This approach has now been used successfully many times to describe long-term changes in Na^+ and Cl^- uptake rates associated with exposure to external environments of altered composition. For example, Evans (1984) has provided a detailed analysis of the relative importance of changes in K_m, J_{max}, and gill permeability in adaptation to different external NaCl levels. Classically, J_{max} is considered an index of the number of transporters present

Abbreviations: Amm total ammonia in water; DMO 5′5-dimethyl-2′4-oxyzolidine-dione; J_{in} unidirectional inward ion movement across the gill; J_{out} unidirectional outward ion movement across the gill; J_{net} net transfer of ions (sum of J_{in} and J_{out}) across the gill; J_{max} maximal transport rate for ion; K_m inverse of affinity of transporter for ion; PIO_2 partial pressure of oxygen in inspired water; P_aCO_2 partial pressure of carbon dixide in arterial blood; TAlk titratable alkalinity of the water; PEG polyethylene glycol; NEN New England Nuclear

[1] *Present address:* Dept. of Biology, University of Ottawa, 30 George Glinski, Ottawa, Ontario, Canada, K1N 6N5.

* To whom offprint requests should be sent

and $1/K_m$ an index of their efficiency. An implicit assumption of this one-substrate Michaelis-Menten model is that the availability of internal counterions (i.e., acidic equivalents for Na^+, basic equivalents for Cl^-) cannot be limiting.

However, very recently it has been shown in freshwater trout that K_m and J_{max} values for Na^+ and Cl^- uptake are also markedly affected by experimental manipulation of internal acid-base status, specifically by metabolic alkalosis induced by either post-hyperoxic recovery (Goss and Wood 1990a) or $NaHCO_3$ infusions (Goss and Wood 1990b). Furthermore, a recent study by Kirschner (1988) on the isolated frog skin has presented convincing evidence that the basis for *apparent* saturation kinetics of Na^+ uptake is the limited availability of the internal acidic counterion (H^+). These observations raise the possibility that the one-substrate Michaelis-Menten model may be overly simplistic in situations where acid-base status is changing. For example, during metabolic acidosis the availability of internal H^+ ions would increase while that of HCO_3^- would decrease. These alterations might result in an increase in Na^+ uptake and a decrease in Cl^- uptake simply by the Law of Mass Action if the concentration of the internal counterion were a rate-limiting influence on the rate of transport. The reverse would be true during metabolic alkalosis. Such a system would represent an automatic, negative feedback control for the clearance/retention of acidic/basic equivalents when acid-base status in changing.

The aim of the present study was to pursue this idea in three ways. The first objective was to characterize the kinetic responses of Na^+ and Cl^- uptake to experimental metabolic acidosis (induced by infusion of isosmotic HCl) in the rainbow trout. These data could then be directly compared to previously published results on experimental alkalosis (Goss and Wood 1990a, b). The second objective was to use the entire data set to evaluate a two-substrate kinetic model which would take into account limitation of Na^+ and Cl^- transport by internal availability of acidic and basic counterions, as represented by extracellular H^+ and HCO_3^- levels. Two-substrate kinetic analysis (Florini and Vestling 1957) is well known in enzymology, but appears not to have been applied to freshwater ion transport. An implicit assumption in this approach (e.g., Kirschner 1988) is that the acid-base status of the extracellular fluid must be reflected in the intracellular fluid bathing the transport sites. Therefore, a final objective was to measure, via a separate series of experiments using the ^{14}C-DMO technique (Milligan and Wood 1986), possible changes in mean gill intracellular pH accompanying the various alkalinizing and acidifying treatments employed in the kinetic experiments.

Materials and methods

Design. This paper presents the results of new experiments on: (i) ion and acid-base transport responses of trout to acid infusion in comparison to non-infused controls; and (ii) the gill intracellular pH responses to acid infusion, base infusion, and post-hyperoxia alkalosis, together with appropriate controls (isosmotic NaCl infusion and no infusion). However, a major focus of the present paper is a comparison of the ion transport kinetics among different groups of trout subjected to each of the above-mentioned treatments, and the application of a two-substrate kinetic model to the complete data set. Therefore, methods were very similar to those previously published, and a portion of the data used in the comparisons and analysis has been taken from those publications (Goss and Wood 1990a, b). Specifically, those data are the ion and acid-base transport result and blood acid-base values for $NaHCO_3$-infused and post-hyperoxia treatments in series I and II below. Additional isosmotic NaCl infusion controls were performed in series I and II in the present study, and found not to differ significantly from values reported earlier (Goss and Wood 1990b); the data sets were therefore combined. In light of this overlap, only a brief description is furnished for previously reported methods; the reader is referred to Goss and Wood (1990a, b) for complete details. In total, experiments were performed on 55 trout in the present study, and additional data were taken from 64 fish studied by Goss and Wood (1990a, b).

The following five treatments were utilized in all three series: (i) control, no infusion; (ii) 140 m*M* NaCl infusion for 10–16 h (2.81 ± 0.10 ml $\cdot$ kg^{-1} $\cdot$ h^{-1} = 393 ± 14 μequiv NaCl $\cdot$ kg^{-1} $\cdot$ h^{-1}); (iii) pure metabolic alkalosis induced by 140 m*M* $NaHCO_3$ infusion for 10–16 h (3.06 ± 0.16 ml $\cdot$ kg^{-1} $\cdot$ h^{-1} = 428 ± 22 μequiv HCO_3^- $\cdot$ kg^{-1} $\cdot$ h^{-1}); (iv) pure metabolic alkalosis induced by return to normoxia ($PIO_2 = 140$ torr) after 72 h exposure to environment hyperoxia ($PIO_2 = 500-550$ torr) – measurements were taken over the 4–8-h period after return to normoxia; and (v) a pure metabolic acidosis induced by 70 m*M* HCl (plus 70 m*M* NaCl) infusion for 10–16 h (2.99 ± 0.13 ml $\cdot$ kg^{-1} $\cdot$ h^{-1} = 210 ± 11 μequiv H^+ $\cdot$ kg^{-1} $\cdot$ h^{-1}) – 70 m*M* HCl rather than 140 m*M* HCl was used because the latter was not tolerated in preliminary experiments.

Preparation of animals. Rainbow trout (*Oncorhynchus mykiss;* 250–400 g) were obtained from Spring Valley Trout Farm, Petersburg, Ontario, Canada and acclimated for at least 2 weeks to 15 ± 1.0 °C in flowing dechlorinated Hamilton tapwater ($Na^+ = 0.6$ mequiv $\cdot$ l^{-1}, $Cl^- = 0.8$ mequiv $\cdot$ l^{-1}, $Ca^{++} = 2.0$ mequiv $\cdot$ l^{-1}, $Mg^{++} = 0.3$ mequiv $\cdot$ l^{-1}, titratable alkalinity [TAlk] = 2.1 mequiv $\cdot$ l^{-1}, pH = 8.0). The fish were starved during the acclimation period to minimize variations in acid output due to feeding. Trout were anaesthetized (MS222, 1:10000) and fitted with a urinary bladder catheter (Wood and Randall 1973) to facilitate separate measurement of branchial fluxes and a dorsal aorta catheter (Soivio et al. 1972) for repetitive blood sampling. Fish were allowed to recover for 48–72 h in aerated, low volume boxes (~ 1.5 l) served with a constant flow of fresh water (~ 0.5 l $\cdot$ min^{-1}).

Acclimation, recovery, experimental series I, and series III were performed in dechlorinated Hamilton tapwater while series II was performed in an prepared NaCl-free media which had the same Ca^{++}, Mg^{++}, TAlk, and pH levels as Hamilton tapwater but lacked Na^+ and Cl^-. Transfer of trout from Hamilton tapwater to this prepared NaCl-free medium does not alter transepithelial potential (Goss and Wood 1990a). The addition of up to 2400 μequiv $\cdot$ l^{-1} NaCl during the kinetic series would likely have negligible effects on transepithelial potential as Ca^{++} and Mg^{++} levels remained the same during this time. Therefore, manipulation of the external NaCl concentration ($[NaCl]_e$) could be performed with little or no alteration of the gill transepithelial potential.

Series I. Series I was designed to measure the "steady-state" exchanges of substances across the gills during each of the five experimental treatments. These included the net branchial fluxes of acidic equivalents ($J_{net}^{H^+}$, as the sum of the titratable and ammonium components), the net branchial fluxes of both ions ($J_{net}^{Na^+,Cl^-}$), and via ^{24}Na and ^{36}Cl radioisotopes, their unidirectional influxes ($J_{in}^{Na^+,Cl^-}$) and outfluxes ($J_{out}^{Na^+,Cl^-}$). Repetitive blood samples (300 μl, with saline replacement) for the analysis of extracellular acid-base status and ions were drawn under control conditions, at 10 and 16 h after the start of the various infusions, or at 3 and 12 h of normoxic recovery.

After 10 h of infusion, or 4 h of post-hyperoxia recovery, water flow to the boxes was stopped and both ^{24}Na (4.0 μCi) and ^{36}Cl (1.0 μCi) were added. After an initial 10-min mixing period, water samples were withdrawn at 0.5-h intervals for 4–6 h and analyzed for $[Na^+]$, $[Cl^-]$, total ammonia (Amm), TAlk, and ^{24}Na and ^{36}Cl cpm. The boxes were flushed after 3 h of closure to ensure that ammonia levels in the water did not exceed 200 μequiv · l^{-1}. Following the flushing, appropriate amounts of isotope were added again to the water.

Series II. Series II was designed to measure the unidirectional uptake kinetics for both Na^+ and Cl^- in fish subjected to the five different experimental regimes. Blood sampling was performed as in series I. After 10 h of infusion, or 4 h of post-hyperoxia recovery, the flow of Hamilton tapwater was stopped and the boxes flushed with NaCl-free water. Uptake kinetic relationships were determined over the following 4 h at nominal $[NaCl]_e$ levels of 50, 150, 300, 600, 1200, and 2400 μequiv · l^{-1}. After an initial 10-min mixing period at each level, samples were taken to begin the flux. After 0.5 h, another sample was withdrawn to end the flux and the $[NaCl]_e$, ^{24}Na and ^{36}Cl were simultaneously increased to the next level by addition from a common 1 *M* NaCl solution. Samples were analyzed for $[Na^+]$, $[Cl^-]$, Amm, TAlk, ^{24}Na and ^{36}Cl cpm.

Series III. Series III was designed to test whether changes in extracellular acid-base status accompanying the five different experimental treatments were reflected in the mean intracellular pH (pH_i) of the gill tissues. Gill pH_i was measured by the ^{14}C–DMO technique (Milligan and Wood 1986; Wright et al. 1988) under control conditions, after approximately 12 h of the various infusions, or after approximately 3 and 12 h of post-hyperoxia recovery. In addition, red blood cell pH_i and white muscle pH_i were also measured for comparison. In each case, the fish was injected with ^{14}C–DMO (5,5-dimethyl-2,4-oxazolidinedione, NEN; 7 μCi · kg^{-1}) and ^{3}H–PEG–400 (polyethylene glycol, MW = 4000, Amersham; 28 μCi · kg^{-1}) via the dorsal aortic catheter approximately 12 h prior to sacrifice. PEG–400 was chosen as an extracellular fluid volume marker after preliminary tests with several other markers (mannitol, inulin, Cl^-–K^+ distribution); PEG was the only one which yielded reliable, reproducible estimates of extracellular space in gill tissue.

Immediately prior to sacrifice, a blood sample (2 ml) was drawn for measurement of blood haemoglobin, red blood cell pH_i, extracellular acid-base status, plasma water content, and plasma ^{14}C–DMO cpm and ^{3}H–PEG cpm. The fish were then killed by a blow on the head. Surface gill tissue (i.e., mainly lamellae and filament surface) was obtained by rapidly removing the gill arches, blotting dry, and then gently scraping the surface of each arch with a glass microscope slide. The tissue obtained was quickly mixed into a homogeneous slurry, an aliquot taken for haemoglobin analysis, and the remainder then processed for determination of ^{14}C–DMO and ^{3}H–PEG cpm and water content. Samples of epaxial white muscle were also processed for these parameters.

Analytical techniques and calculations. Calculations for ion and acid-base fluxes in series I and II were identical to those of Goss and Wood (1990a, b), and analytical techniques were generally comparable. In brief, water $[Na^+]_e$ was measured by atomic absorption, water $[Cl^-]_e$ by the mercuric thiocyanate method (Zall et al. 1956) and water [Amm] by the sacylate-hypochlorite method (Verdouw et al. 1978). Titratable alkalinity was determined as described by McDonald and Wood (1981). Duplicate 5-ml water samples were assayed for the sum of ^{36}Cl and ^{24}Na cpm by scintillation counting immediately following the end of the experiment. The ^{24}Na isotope was allowed to decay for at least 50 half-lives (half-live = 14.96 h) and the sample was recounted assuming that only ^{36}Cl (half-life = 300000 years) remained. The ^{24}Na cpm were obtained by subtraction and decay correction.

Blood samples were drawn anaerobically; arterial pH_a and plasma total CO_2 were determined immediately by standard Radiometer techniques (Wood and Jackson 1980). The P_aCO_2 and plasma HCO_3^- levels were calculated by rearrangement of the Henderson-Hasselbalch equation using the values of pK' and αCO_2 tabulated in Boutilier et al. (1984).

In series II, the relationship between $[NaCl]_e$ and the influx of either Na^+ or Cl^- followed distinctive saturation kinetic curves that were characterized initially by Michaelis-Menten analysis. The curves fitted to the uptake kinetic data (Fig. 2) were generated by substitution into the one-substrate Michaelis-Menten equation:

$$J_{in}^X = \frac{J_{max} \cdot [X]_e}{K_m + [X]_e} \quad (1)$$

using the mean values for K_m and J_{max} from all individual fish in a particular treatment. Here X is the ion in question (Na^+ or Cl^-), J_{in}^X is the influx rate at a particular external $[X]_e$, K_m is the inverse of affinity, and J_{max} is the maximal rate of transport. Both K_m and J_{max} were determined for each fish via transformation of the data by Eadie-Hofstee regression analysis (Michal 1985). This one-substrate analysis comprised the first step in the more complex two-substrate analysis (Florini and Vestling 1957) which is described in detail in the Discussion.

In series III, equations for calculating intra- and extracellular fluid volumes and pHi were identical to those given by Milligan and Wood (1986) and Wright et al. (1988), and analytical methods were generally comparable. In brief, ^{14}C–DMO and ^{3}H–PEG cpm were separated by dual-label quench correction using quench standards prepared from gill and white muscle homogenates, and the external standard-ratio method. Haemoglobin was measured by the cyanmethaemoglobin technique (Blaxhall and Daisley 1973), plasma water content by refractometry (Alexander and Ingram 1980), tissue water content by drying to a constant weight at 85 °C, extracellular pH (arterial blood pHa) by a Radiometer capillary electrode, and red blood cell pH_i by the freeze-thaw lysate method (Zeidler and Kim 1977) with the same electrode. Gill intracellular fluid volumes and pH_i values were corrected for the presence of trapped red cells based on the measured haemoglobin content of the gill homogenate.

Statistical analyses. All values are presented as means ± 1 SEM (*n*). Comparisons between two independent means were tested by Student's unpaired two-tailed *t*-test. Comparisons among multiple means were performed by a one-way analysis of variance (ANOVA), followed by Duncan's new multiple range test to determine invidual differences in cases where the *F*-value of the ANOVA indicated significance. A significance level of $P < 0.05$ was employed throughout.

Results

Extracellular acid-base status (series I and II) was relatively stable over the measurement periods of the five different experimental treatments; mean values are summarized in Table 1. HCl infusion resulted in a significant fall in arterial pH; this acidosis was purely metabolic in origin as P_aCO_2 remained unchanged while plasma $[HCO_3^-]$ was reduced by 35% (Table 1). NaCl infusion had no significant effect on blood acid-base status. Both $NaHCO_3$ infusion and post-hyperoxia recovery induced almost pure metabolic alkaloses. Arterial pH was significantly elevated relative to both control and NaCl treatments due to 100–150% elevations in plasma $[HCO_3^-]$ with only slight increases in P_aCO_2.

"Steady-state" exchange rates of ions and acid-base equivalents at the gills (series I) were also relatively stable during the five experimental treatments; mean values averaged over the entire measurement periods (10–16 h

infusion, 4–8 h post-hyperoxia) are presented in Fig. 1. Under control conditions, fish were in approximate zero balance for Na^+, Cl^-, and acidic equivalent fluxes at the gills.

Infusion of HCl resulted in differential changes in Na^+ and Cl^- transport. $J_{in}^{Na^+}$ increased by 100% relative to the control group, with no change in $J_{out}^{Na^+}$, resulting in a large net gain of Na^+ (Fig. 1A, *shaded bars*). This increase in $J_{in}^{Na^+}$ was also significant relative to the NaCl group. In contrast, $J_{in}^{Cl^-}$ decreased slightly during HCl infusion while $J_{out}^{Cl^-}$ showed a tendency to increase (Fig. 1B). These non-significant effects combined to result in a significant loss of Cl^- in the HCl infused group compared to the control group. In view of this net loss of anion (Cl^-) and gain of cation (Na^+), a net branchial excretion of acidic equivalents would be predicted by the constraints of electroneutrality. Indeed, Fig. 1C shows that HCl-infused trout exhibited a net acidic equivalent loss of about -200 μequiv · kg^{-1} · h^{-1} across the gills which almost exactly matched the H^+ infusion rate ($+210$ μequiv · kg^{-1} · h^{-1}). This indicates that the fish had reached a relatively steady state over the 10–16-h period. Negative $J_{net}^{H^+}$ was achieved by a marked reduction in J^{TA} and a significant increase in J^{Amm}.

NaCl infusion had negligible effect on gill acidic equivalent fluxes although net Na^+ and Cl^- fluxes both became negative. In fish loaded with isosmotic NaCl at a rate of $+410$ μequiv · kg^{-1} · h^{-1}, there was a simultaneous net excretion of both Na^+ and Cl^- at approximately -200 μequiv · kg^{-1} · h^{-1}, achieved mainly through a stimulation of the J_{out} components (Fig. 1A, B). Therefore, there was no differential net flux of cations *versus* anions and thus no net acidic equivalent gain/excretion (Fig. 1C).

$NaHCO_3$ infusion and post-hyperoxia treatments induced similar effects on ion and acidic equivalent fluxes, with differences only in the magnitude of the response, which was larger in the $NaHCO_3$ treatment. Alkalosis was associated with a net Na^+ loss and a net Cl^- gain, mainly through alterations in the influx components. $J_{in}^{Na^+}$ was reduced by 40–70% (Fig. 1A) and $J_{in}^{Cl^-}$ increased by 35–45% (Fig. 1B) in comparison to the control group. These changes were also significant relative to the NaCl treatment. The net gain of anions and loss of cations would be expected to reduce the SID therefore result in a gain in acidic equivalents (or loss of basic equivalents). In accord with prediction, $J_{net}^{H^+}$ was highly positive in both alkalotic groups (Fig. 1C). In the $NaHCO_3$ treatment, net acidic equivalent uptake was about

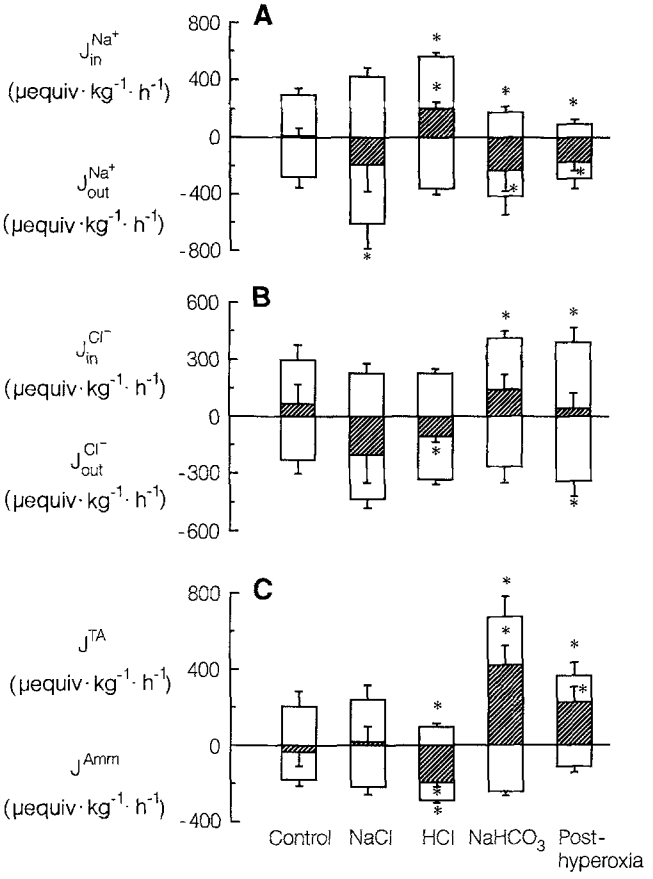

Fig. 1A–C. Mean unidirectional influx (J_{in}), outflux (J_{out}), and net flux *(shaded bars)* for (**A**) Na^+, (**B**) Cl^-, and (**C**) the flux or titratable acidity (J^{TA}), ammonia (J^{Amm}), and net acidic equivalents *(shaded bars)* under five experimental conditions of series I: (i) control, no infusion ($n=16$); (ii) 140 m*M* NaCl infusion for 10–16 h (2.81 ± 0.10 ml · kg^{-1} · h^{-1} = 393 ± 14 μmol NaCl · kg^{-1} · h^{-1}, $n=8$); (iii) 70 m*M* HCl (plus 70 m*M* NaCl) infusion for 10–16 h (2.99 ± 0.13 ml · kg^{-1} · h^{-1} = 210 ± 11 μequiv H^+ · kg^{-1} · h^{-1}, $n=6$); (iv) 140 m*M* $NaHCO_3$ infusion for 10–16 h [3.06 ± 0.16 ml · kg^{-1} · h^{-1} = 428 ± 22 μequiv HCO_3^- · kg^{-1} · h^{-1}, $n=7$ (Goss and Wood 1990b)]; (v) return to normoxia ($PIO_2=140$ torr) after 72 h exposure to environmental hyperoxia [$PIO_2=50$–550 torr, $n=10$ (Goss and Wood 1990a)]. *Asterisks* (*) indicate significant difference from control ($P<0.05$). See text for additional details. Means ± 1 SEM

$+220$ μequiv · kg^{-1} · h^{-1}, virtually identical to the HCO_3^- infusion rate (-228 μequiv · kg^{-1} · h^{-1}), indicating that a steady state was achieved by 10–16 h of infusion. In the post-hyperoxic fish, $J_{net}^{H^+}$ reached only half

Table 1. Arterial blood acid-base in rainbow trout under the five experimental treatments. Means ± 1 SEM

Treatment	(*n*)	pH_a	$[HCO_3^-]_a$ (mequiv · l^{-1})	P_aCO_2 (torr)
Control	(16)	7.907 ± 0.018	7.10 ± 0.42	2.17 ± 0.10
NaCl	(10)	7.884 ± 0.033	8.20 ± 1.47	2.35 ± 0.04
HCl	(14)	7.740 ± 0.029* **	4.54 ± 0.35* **	1.94 ± 0.15
$NaHCO_3$[a]	(13)	8.161 ± 0.025* **	18.21 ± 2.26* **	2.75 ± 0.36*
Post-hyperoxia	(10)	8.084 ± 0.038* **	14.21 ± 1.57* **	2.84 ± 0.13* **

* = significantly different from control group ($P<0.05$)
** = significantly different from NaCl group ($P<0.05$)
[a] From Goss and Wood (1990b)

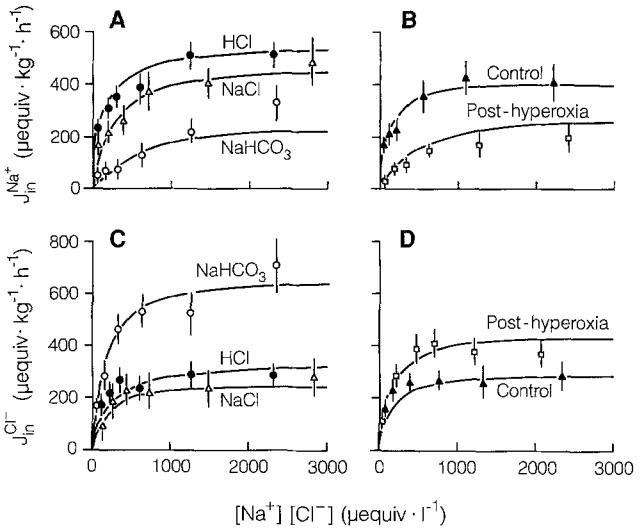

Fig. 2A–D. The kinetics of (**A, B**) Na^+ influx and (**C, D**) Cl^- influx as a function of external Na^+ or Cl^- concentrations, respectively, in rainbow trout exposed to the five experimental conditions in series II. (i) control ($n=16$); (ii) 140 m*M* NaCl infusion, $n=7$; (iii) 70 m*M* HCl (plus 70 m*M* NaCl) infusion, $n=8$; (iv) 140 m*M* $NaHCO_3$ infusion, $n=7$ (Goss and Wood 1990b); (v) return to normoxia ($PIO_2=140$ torr) after 72 h exposure to environmental hyperoxia ($PIO_2=500$–550 torr), $n=12$ (Goss and Wood 1990a). Curves were drawn by Michealis-Menten analysis from mean estimates of K_m and J_{max} by Eadie-Hofstee regression analysis for all individual fish in each group. Mean J_{in} values have been plotted at mean $[Na^+]$ or $[Cl^-]$ values for each point. See text for further details. Means ± 1 SEM

this rate, reflecting the smaller metabolic alkalosis (Table 1). In both treatments, the increase in $J_{net}^{H^+}$ reached only half this rate, reflecting the smaller metabolic alkalosis (Table 1). In both treatments, the increase in $J_{net}^{H^+}$ resulted from a stimulation of J^{TA}; J^{Amm} did not change significantly (Fig. 1C) from control fish.

The results of series I demonstrated that branchial flux rates were relatively stable at 10–16 h infusion and 4–8 h post-hyperoxia. These periods were therefore chosen for the kinetic experiments of series II. The uptake kinetic curves were obtained by sequentially increasing water $[NaCl]_e$ and monitoring the rates of $J_{in}^{Cl^-}$ and $J_{in}^{Na^+}$. For the sake of clarity, Figs. 2A and 2B show the relationships for fish infused with NaCl, HCl and $NaHCO_3$, while Figs. 2C and 2D compare the relationships for control (non-infused) and post-hyperoxia treatments. The lines fitted to the data are based on the Michaelis-Menten model for one-substrate reactions using the mean values of K_m and J_{max} obtained for each individual fish by Eadie-Hofstee regression (see Table 2). In general, the experimentally determined relationships between $J_{in}^{Na^+}$ and $[Na^+]_e$, and between $J_{in}^{Cl^-}$ and $[Cl^-]_e$ were well described by one-substrate analysis. Comparison of the rates of $J_{in}^{Na^+}$ and $J_{in}^{Cl^-}$ at mean water $[Na^+]_e=600$ μequiv · l^{-1} and $[Cl^-]_e=800$ μequiv · l^{-1} predicted by these kinetic curves from series II (Fig. 2) with the "steady state" influx rates measured at these concentrations in series I (Fig. I) shows relatively good agreement for all treatment groups.

The positions of the kinetic uptake curves varied as a function of the extracellular acid-base status (Fig. 2). Thus, the Na^+ uptake curve was displaced upwards by HCl infusion and markedly downwards by the two alkalotic treatments ($NaHCO_3$ infusion and post-hyperoxia), in comparison to the two acid-base neutral treatments (control and NaCl infusion; Fig. 2A, C). In contrast, the Cl^- uptake relationship was shifted dramatically upwards by the $NaHCO_3$ infusion, and to a lesser extent by the post-hyperoxia treatment. However, HCl infusion had no definite effect on the position of the Cl^- uptake relationship. There were no apparent differences in the uptake rates for Cl^- at any of the external Cl^- concentrations among HCl-infused fish, NaCl-infused fish, and control fish (Fig. 2B, D).

The mean K_m and J_{max} values for these curves from the one-substrate Michaelis-Menten model are tabulated in Table 2. HCl infusion had no effect on $K_m^{Na^+}$ relative to the non-infused control fish. However since $K_m^{Na^+}$ was significantly elevated (i.e., affinity decreased) by NaCl infusion, the value in the HCl infused group was significantly lower than in this sham treatment. Much larger 5–6 fold increases in $K_m^{Na^+}$ were seen in the two alkalotic treatments, $NaHCO_3$ infusion and post-hyperoxia. There were no significant differences in $K_m^{Cl^-}$ among the five treatments, though HCl infusion caused a small, non-significant elevation. A simple interpretation of these patterns is that the Na^+ and Cl^- uptake systems normally operate close to their maximum affinities (i.e., minimum K_m) for the external substrates. Affinity can apparently be decreased for the purposes of acid-base correction, but cannot be increased above controls levels.

In contrast, J_{max} values by one-substrate analysis (Table 2) can apparently be either increased or decreased

Table 2. Mean estimates of K_m and J_{max} obtained by one-substrate Michaelis-Menten analysis for the Na^+ and Cl^- transporters in rainbow trout gills under the five experimental treatments. Means ± 1 SEM

Treatment	(*n*)	K_m Na^+ (μequiv · l^{-1})	K_m Cl^- (μequiv · l^{-1})	J_{max} Na^+ (μequiv · kg^{-1} · h^{-1})	J_{max} Cl^- (μequiv · kg^{-1} · h^{-1})
Control	(8)	99 ± 15	127 ± 20	420 ± 52	286 ± 27
NaCl	(9)	191 ± 28*	121 ± 13	480 ± 80	303 ± 68
HCl	(8)	105 ± 15**	178 ± 53	548 ± 51*	336 ± 39
$NaHCO_3$[b]	(6)	463 ± 82* **	135 ± 12	262 ± 43* **	674 ± 89* **
Post-hyperoxia[a]	(12)	559 ± 52* **	137 ± 13	310 ± 65* **	445 ± 54*

* = significantly different from control group ($P<0.05$)
** = significantly different from NaCl group ($P<0.05$)
[a] From Goss and Wood (1990a)
[b] From Goss and Wood (1990b)

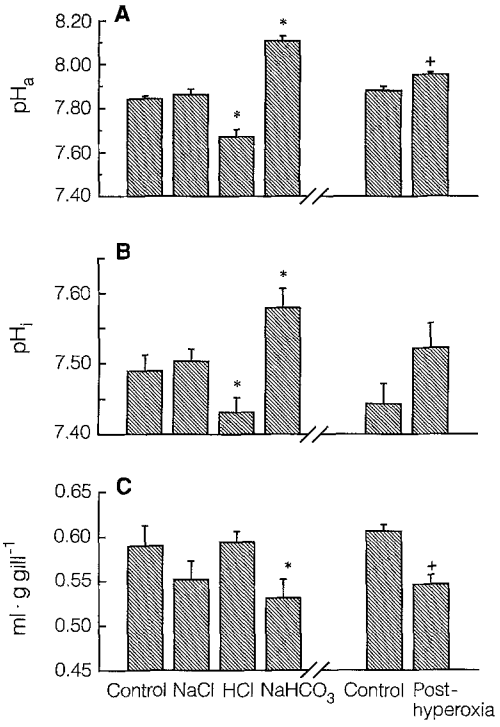

Fig. 3A–C. Mean values of (**A**) arterial pH, (**B**) gill cell intracellular pH, and (**C**) extracellular fluid volume under the five experimental conditions in series III. (i) control, $n=8$; (ii) 140 m*M* NaCl infusion, $n=7$; (iii) 70 m*M* HCl (plus 70 m*M* NaCl) infusion, $n=7$; (iv) 140 m*M* $NaHCO_3$ infusion, $n=7$; (v) normoxic control for hyperoxia experiments, $n=18$; and (vi) return to normoxia ($PIO_2=140$ torr) after 72 h exposure to environmental hyperoxia ($PIO_2=550$–550 torr, $n=15$. Note that a separate control group was measured for the post-hyperoxic treatment. Note that the *y*-axis range in Fig. 3B is much narrower than in Fig. 3A. Means ± 1 SEM. * indicates significantly different from control fish, + indicates significantly different from hyperoxic control fish ($P<0.05$)

relative to control values for the purposes of acid-base correction. Thus $J_{max}^{Na^+}$ was elevated 30% by acidosis (HCl infusion) and depressed 30–40% by alkalosis ($NaHCO_3$ infusion and post-hyperoxia). NaCl infusion had no effect. $J_{max}^{Cl^-}$ was unaffected by acidosis or NaCl infusion, but was elevated 55% (post-hyperoxia) and 135% ($NaHCO_3$) by the two alkalotic treatments. Classically, these changes in J_{max} determined by one-substrate Michaelis-Menten analysis would be interpreted as alterations in the number of transporters present. However, two-substrate analysis provides a fundamentally different interpretation (see Discussion).

Series III tested whether changes in extracellular acid-base status were reflected in the intracellular compartment of the gill tissue (Fig. 3). Note that a separate normoxic control was performed for the post-hyperoxia treatment in this series because these hyperoxia experiments were conducted at a different time than the others. Gill extracellular spaces, measured by PEG–4000 distribution, were elevated by $NaHCO_3$ infusion and post-hyperoxia; as total gill water (0.8394 ± 0.0018 ml · g^{-1}) did not change, mean intracellular fluid volume fell significantly in these two alkalotic treatments (Fig. 3C). NaCl and HCl infusions had no effect on gill fluid volume

Table 3. Intracellular pH of the red blood cells (RBC pH_i) and white muscle (WM pH_i) in rainbow trout under the five experimental treatments. Means ± 1 SEM

Treatment	(*n*)	RBC pH_i	WM pH_i
Control	(8)	7.311 ± 0.012	7.309 ± 0.010
NaCl	(7)	7.314 ± 0.015	7.342 ± 0.022
HCl	(7)	7.250 ± 0.008**	7.319 ± 0.022
$NaHCO_3$	(7)	7.423 ± 0.031**	7.442 ± 0.031**
Normoxic control	(18)	7.313 ± 0.016	7.301 ± 0.018
Post-hyperoxia	(15)	7.325 ± 0.013	7.465 ± 0.025***

* = significantly different from control $P<0.05$
** = significantly different from NaCl-infused $P<0.05$
*** = significantly different from normoxic control $P<0.05$

distribution. Changes in extracellular pH_a (Fig. 3A) and HCO_3^- and P_aCO_2 (not shown) in the five experimental treatments were similar to those seen in series I and II (Table 1).

Mean gill cell pH_i (Fig. 3B) qualitatively followed the trends noted for extracellular pH_a (Fig. 3A), though the absolute changes were smaller. Thus, in the face of extracellular pH_a depression of about 0.20 pH units during HCl infusion, gill pH_i fell significantly by about 0.06 units. Similarly during $NaHCO_3$ infusion, pH_a rose by about 0.25 units, and gill pH_i increased significantly by about 0.07 units. A comparable, though non-significant, rise in gill pH_i occurred in post-hyperoxia. NaCl infusion had no effect. By way of comparison, mean gill pH_i was 0.15–0.20 units higher than either red blood cell or white muscle pH_i values (Table 3). In general, pH_i trends during acid-base disturbance were similar in all three tissues, though white muscle pH_i did not fall during HCl infusion, and red blood cell pH_i did not rise during post-hyperoxia (Table 3).

Discussion

Acidosis, alkalosis, and one-substrate analysis. The present study on HCl infusion and the data from Goss and Wood (1990a, b) support the idea that fish actively modulate their branchial ionic exchangers to regulate blood acid-base status (Wood et al. 1984; Claiborne and Heisler 1984, 1986; Perry et al. 1987; Wood 1988). A metabolic acidosis induced by chronic HCl infusion resulted in an elevated $J_{in}^{Na^+}$ while $J_{in}^{Cl^-}$ remained unchanged, whereas a metabolic alkalosis induced by chronic $NaHCO_3$ infusion or post-hyperoxic recovery resulted in a reduced $J_{in}^{Na^+}$ and an elevated $J_{in}^{Cl^-}$. Net branchial Na^+ flux was positive during acidosis and negative during alkalosis, while exactly the opposite was true for Cl^-. In all cases, the difference between $J_{net}^{Na^+}$ and $J_{net}^{Cl^-}$ was virtually equivalent to the net flux of acidic equivalents in the opposite direction (Fig. 1).

However, the mechanisms by which fish regulate the transporters present on the gill surface appear complex. In HCl-infused fish, there were significant increases in

$J_{max}^{Na^+}$ while $K_m^{Na^+}$, $J_{max}^{Cl^-}$, and $K_m^{Cl^-}$ remained unchanged. Classical interpretation of these results would be that the number of Na^+ transporters increased, while number of Cl^- transporters remained unchanged (Shaw 1959; Evans 1984). The lack of an increase in affinity (decrease in K_m) supports the hypothesis put forward by Goss and Wood (1990b) that the affinity of the transporters ($1/K_m^{Na^+}$, $1/K_m^{Cl^-}$) for the external ion operates at or near maximum under control conditions and cannot be increased by acid-base stimuli in order to achieve a greater uptake of ions. However, affinity can clearly be decreased (K_m increased), as seen for $K_m^{Na^+}$ in the $NaCHO_3$-infused and post-hyperoxic groups. In addition, classical interpretation of the fall in $J_{max}^{Na^+}$ and rise in $J_{max}^{Cl^-}$ in these groups would be that the number of transporters decreased and increased, respectively.

Regulation of J_{max} is clearly an important phenomenon for adjustments of ion and acidic equivalent fluxes during acid-base disturbances. If this is accomplished by alteration of the number of transport sites, several possible mechanisms could be involved. These include: (1) an altered synthesis of the transport proteins in the cell (Evans 1984); (2) the insertion/deletion of transporters into the epithelial membrane from cytoplasmic vesicles as has been shown for H^+ pumps in the turtle bladder (Stetson and Steinmetz 1983); (3) the activation/deactivation of nascent transporters already present on the membrane surface (Frain 1987); and (4) the addition/removal of new transport cells to the gill epithelium (Avella et al. 1987; Perry and Laurent 1989; Laurent and Perry 1990). These mechanisms would act to effectively increase/decrease the rate of uptake of the ion and the associated acidic or basic equivalent efflux.

Two-substrate analysis. However, there exists an alternative, fundamentally different explanation for variations in $J_{max}^{Na^+}$ and $J_{max}^{Cl^-}$ during acid-base disturbances – specifically that these adjustments are due to changes in the internal availability of a limiting acidic or basic counterion. For example, Kirschner (1988), working on isolated frog skin, measured $J_{in}^{Na^+}$ at a level of $[Na^+]_e$ that was thought to be a saturating concentration. Short circuiting the skin or buffering the mucosal solution was found to increase $J_{in}^{Na^+}$ up to three-fold due the dissociation of the electrical coupling between H^+ excretion and Na^+ uptake. This demonstrated that the apparent saturation of Na^+ uptake from fresh water resulted from limitation of the efflux of the internal counterion (nominally H^+) to the water. An implicit assumption of the one-substrate model utilized by previous workers is that the availability of the counterion cannot limit the rate of transport. Kirschner's results challenge a basic premise of the one-substrate Michaelis-Menten model.

A two-substrate model which recognizes the condition that the concentration of *either* of the two substrates (i.e., external Na^+ and internal H^+, external Cl^- and internal HCO_3^-) may be limiting was developed in enzyme biochemistry a number of years ago (Florini and Vestling 1957). Michal (1985) provides a detailed description. To date, this model does not appear to have been employed in the field of ion and acid-base transport in fish. A major objective of the present study was to test applicability of this model to the analysis of dynamic changes in branchial Na^+, Cl^-, and acid-base exchange in the freshwater trout.

The two-substrate model requires estimates of the *apparent* K_m and J_{max} for the Na^+ and Cl^- transporters. These are the values generated from a one-substrate Michaelis-Menten analysis presented previously. The terms "*apparent* K_m" and "*apparent* J_{max}" will be used to describe the values obtained by one-substrate analysis when the internal [counterion] is limiting on the rate of transport of the external ion. "*True* K_m" and "*true* J_{max}" as calculated by the two-substrate analysis represent the kinetic parameters when both the internal and external substrate for the transporter are present in saturing concentrations. *True* J_{max} and *true* K_m values are indicated by an asterisk (*) in Figs. 4 and 5.

In addition to the measurements of *apparent* K_m and *apparent* J_{max} for each of the transporters, measurements of the acid-base status of the fish are required as indices of internal counterion concentrations. In the following analysis, we have utilized the extracellular acid-base status. If as believed (McDonald and Prior 1988; Avella and Bornancin 1989), the transporters are located on the apical membranes of the branchial transport cells, then it could be legitimately argued that the intracellular acid-base status of these cells should be used in this analysis. However, such data are not available, and indeed, have never been measured in freshwater fish. Mean gill pH_i measurements (Fig. 3) are viewed as estimates for the whole surface tissue of the gill, of which the transport cells are only one component. Furthermore, the nature of HCO_3^- distribution between extracellular and intracellular fluid in the gill tissue is unknown.

Nevertheless, we believe that the use of extracellular acid-base data in the present analysis is valid for the following reasons: (1) the net effect of the branchial transport systems is to achieve a 1:1 exchange of Na^+ against acidic equivalents and Cl^- against basic equivalents between the external water and the extracellular fluid; (2) gill pH_i qualitatively followed the measured extracellular pH_a in each of the acid-base disturbances utilized (Fig. 3); and (3) in the isolated frog skin, Ehrenfeld et al. (1985) and Kirschner (1988) have shown that the net H^+ flux is directly correlated with the pH gradient from serosal (extracellular) to mucosal (water) sides. As in these studies, it is assumed that changes in extracellular acid-base status are reflected in intracellular acid-base status, and that the system is acting to regulate the pH in the extracellular compartment.

The relationship between the uptake of an external substrate (e.g., $J_{in}^{Cl^-}$ or $J_{in}^{Na^+}$) and the simultaneous efflux of the internal substrate ($J_{out}^{HCO_3^-}$ $J_{out}^{H^+}$) can be described by the following equation (Florini and Vestling 1957) which is the equation for both the one-substrate Michaelis-Menten analysis and the novel two-substrate analysis:

$$J_{in} = \frac{J_{max}^*}{1 + \frac{(K_m)S_1^*}{[S_1]} + \frac{(K_m)S_2^*}{[S_2]} + \frac{(K_m)S_1S_2}{[S_1][S_2]}} \quad (2)$$

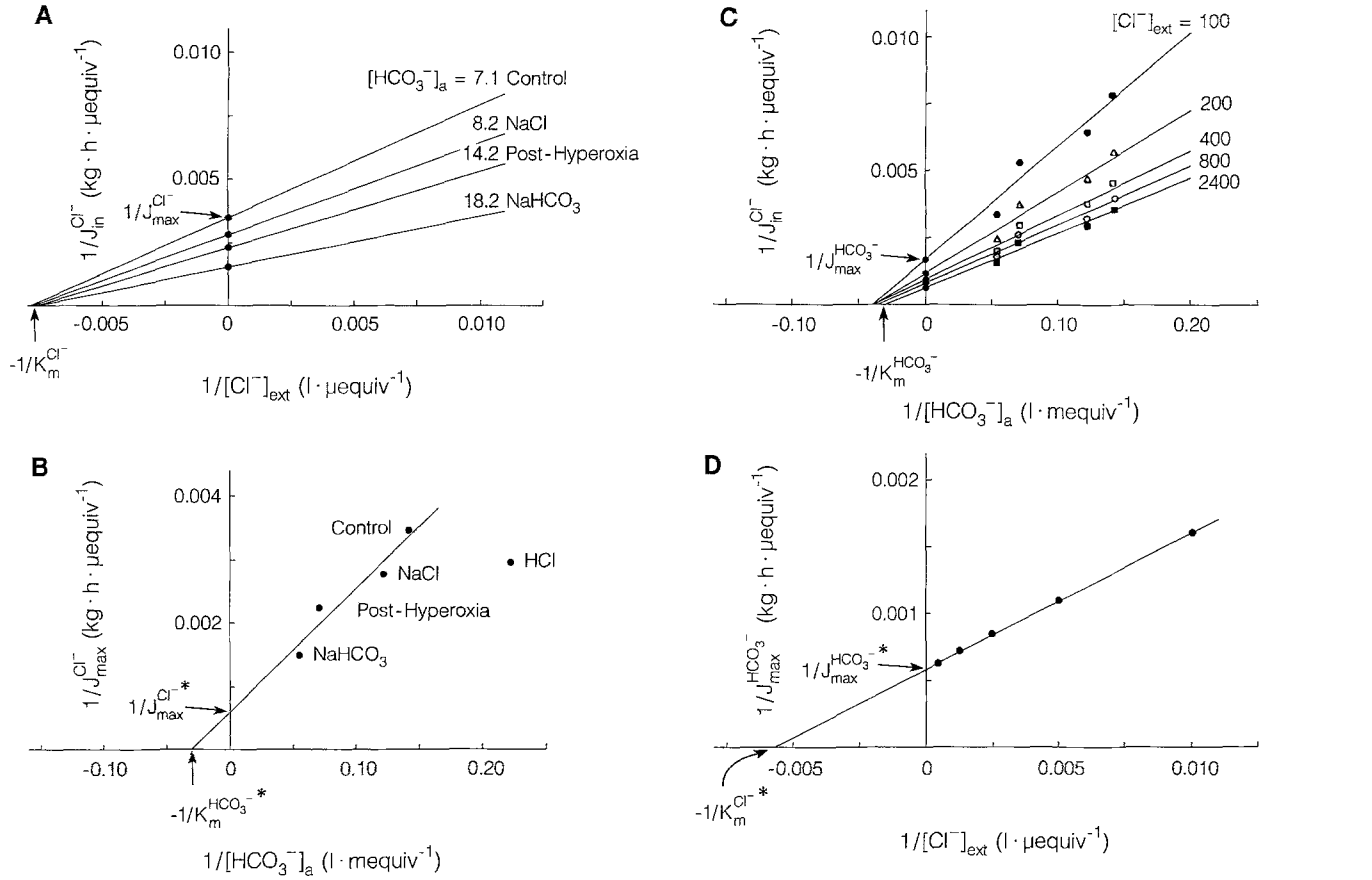

Fig. 4A–D Two-substrate kinetic analysis for the branchial Cl^-/HCO_3^- exchange system in rainbow trout. Mean data from four of the five experimental treatments were used in the analysis. HCl infusion was omitted. See text for detailed explanation

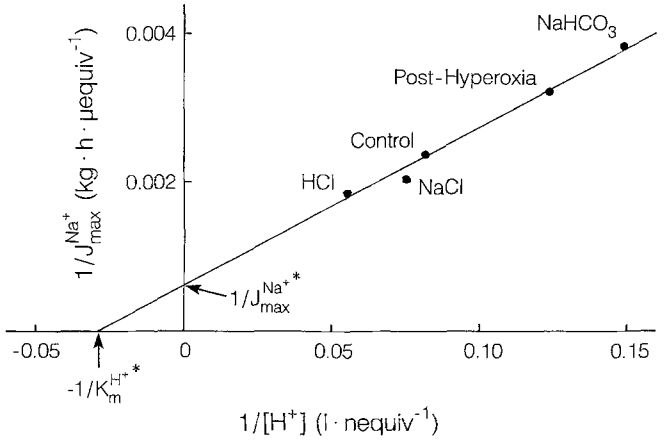

Fig. 5. Second panel of the two-substrate kinetic analysis for the branchial Na^+/H^- exchange system in rainbow trout. Mean data from all five experimental treatments were used in the analysis. See text for detailed explanation

Here S_1 and S_2 are the concentrations of external substrates ($[Cl^-]$ or $[Na^+]$) and internal substrates ($[HCO_3^-]$ or $[H^+]$) respectively. $(K_m)S_1S_2$ is a compound term describing the affinity/dissociation of the transporter/two substrate complex while $(K_m)S_1^*$ and $(K_m)S_2^*$ are the *true* estimates of the affinity/dissociation constants of the transporter for each of the substrates separately. *True* J_{max}^* is the transport rate when both the internal and external substrate are present in unlimiting concentrations, i.e., concentrations much greater than the corresponding *true* $(K_m)S_1^*$ and *true* $(K_m)S_2^*$.

The one-substrate analysis utilized previously assumes that the concentration of the internal counterion (S_2) is not limiting J_{in}. Thus, in equation 2, $[S_2]$ would be much larger than *true* $(K_m)S_2^*$, both the second and third terms in the denominator would become vanishingly small, and Eq. (2) would simplify to:

$$J_{in} = \frac{J_{max}^*}{1 + \frac{(K_m)S_1^*}{[S_1]}} \quad (3)$$

which is just a rearrangement of the Michaelis-Menten equation (1). If however, *true* $(K_m)S_2^*$ is close to or greater than the actual concentration of the internal counterion $[S_2]$, then both the second and third term of the denominator will be significant and the concentration of S_2 will play a critical role in the determination of J_{in}.

The analysis is complex and, therefore, will be explained in detail with reference to Figs. 4A–D which utilize the present data set for the analysis of the Cl^-/HCO_3^- exchange system. In general, the experimental data fitted this model extremely well.

The first step (Fig. 4A) is a standard Lineweaver-Burk or double reciprocal plot for determination of *apparent* K_m and *apparent* J_{max} values in a one-substrate analysis. However, according to the two-substrate model, the slope of each line, and hence the *y*-intercept or *apparent* $J^{S_1}_{max}$, is not determined by the number of transporters, but rather by the concentration of the internal counterion $[S_2]$. Thus as internal $[HCO_3^-]$ increases, $1/J^{Cl^-}_{max}$ decreases (i.e., *apparent* $J^{Cl^-}_{max}$ increases).

The second step (Fig. 4B) is a double reciprocal plot of the *apparent* J_{max} (*y*-intercept) values generated in the first step versus the respective $[S_2]$ values. Therefore, as internal $[HCO_3^-]$ becomes infinitely large, $1/[HCO_3^-]$ becomes infinitely small and intercept on the y-axis yields *true* $J^{Cl^-*}_{max}$. The *x*-intercept provides an estimate of the *true* $(K_m)S_2^*$ and therefore the affinity of the transporter for the internal counterion (HCO_3^-), an estimate which cannot be determined by one-substrate analysis. Note however, that the HCl infusion data did not fall on the same relationship as the other four treatments, and therefore were not used in the analysis. The probable reason for this discrepancy will be discussed below.

The third step (Fig. 4C) is directly analogous to the first step. However, now the concentration of the external substrate $[S_1]=[Cl^-]_e$ is set to several constant values. Flux rates are calculated using the values of *apparent* K_m and *apparent* J_{max} determined in the first step (Fig. 4A, Table 2) for each of the treatments (i.e., different $[S_2]=[HCO_3^-]$ values). A double reciprocal plot of flux rate versus $[S_2]$ will yield estimates of *apparent* $J^{HCO_3^-}_{max}$ from the *y*-intercept and *apparent* $K_m^{HCO_3^-}$ from the *x*-intercept. However, the slope of each line is now determined by the external substrate concentration ($[S_1]$).

The fourth and final step is analogous to the second step. Values for *true* $J^{S_2^*}_{max}$ and *true* $(K_m)S_1^*$ are determined by making double reciprocal plots of the *apparent* $J^{S_2}_{max}$ values generated in the third step versus the $[S_1]$. Therefore, as $[Cl^-]_e$ becomes infinitely large, $1/[Cl^-]_e$ becomes infinitely small and the intercept of the *y*-axis will yield *true* $J^{HCO_3^-*}_{max}$. The *x*-intercept provides an estimate of the *true* $K_m^{Cl^-*}$ or the real affinity of the transporter for the external counterion (Cl^-). Comparison of the *x*-intercepts of Figs. 4B and 4D demonstrated that $J^{HCO_3^-*}_{max}$ and $J^{Cl^-*}_{max}$ estimates are virtually identical (i.e., 1-for-1 exchange), while $K_m^{HCO_3^-*}$ and $K_m^{Cl^-*}$ differ from one another by several orders of magnitude.

Figure 5 shows the application of the model to the Na^+/H^+ transport system; the analysis was only feasible up to the second step. In step three, double reciprocal plots of the calculated flux rates (at various constant values of $[Na^+]_e$) against internal $[H^+]$ were curvilinear, the slope progressively decreasing as the *y*-axis was approached, i.e., at lower pH_a, the calculated flux rates were higher than expected and vice versa. Assuming that the two-substrate approach is valid for Na^+ transport, two explanations are possible. The first is artifact, since small errors in the measurement of pH correspond to large errors when $[H^+]$ is put on a linear scale. The second is that H^+ may not be the only internal substrate for the Na^+ transport system. Kirschner (1988) did not always find a strict coupling between H^+ efflux and Na^+ uptake in the isolated frog skin and suggested that a significant portion of the Na^+ uptake was coupled to the extrusion of another (unidentified) cation. An obvious possibility for the other internal substrate in the fish gill would be NH_4^+ (Maetz 1972, 1973; Kirschner et al. 1973; Wright and Wood 1985; McDonald and Prior 1988). Since NH_4^+, like H^+, represents an acidic equivalent, use of the two-substrate model linking ion and acid-base transport would still be valid. Unfortunately, internal $[NH_4^+]$ was not measured in the present studies, although it is interesting that measured J^{Amm} was greatest in the HCl-infused treatment (Fig. 1C), which were the fish with lowest pH_a (Table 1). Clearly, further work is needed to separate these two possibilities.

An alternative explanation for the curvilinearity of the third step in the execution of the two-substrate model for the Na^+ uptake/H^+ excretion mechanism is that the exchange system may not be a directly coupled two-site protein, for which the model is designed. Avella and Bornancin (1989) recently proposed that the system for Na^+ uptake in freshwater fish may be operating using an H^+-ATPase (H^+ pump) electrochemically coupled to the Na^+ uptake by the apical membrane potential as has been found for frog skin (Ehrenfeld et al. 1985), rather than an electroneutral Na^+/H^+ exchanger. However, it remains to be demonstrated if either or both of these mechanisms are involved in the uptake of Na^+ in freshwater fish.

Results of the two-substrate analysis are listed in Table 4 which compares the *true* K_m^* and J_{max} values for both the Cl^-/HCO_3^- exchange and Na^+ transporters with the respective *apparent* values as calculated by one-substrate Michaelis-Menten model. It must be remembered that these estimates were gained from the use of extracellular values for acidic and basic equivalent concentrations for the performance of the two-substrate analysis. Only intracellular analysis, which is not possible with present technology, can provide true estimates for each of these parameters. The present analysis relies on the assumption that intra- and extracellular acid-base status are at least qualitatively linked. Despite this limitation, an important contribution of the two-substrate model is that it yields estimates of *true* $K_m^{H^+*}$ and $K_m^{HCO_3^-*}$, values which have not been estimated previously in freshwater fish. *True* $J^{HCO_3^-*}_{max}$ and *true* $J^{Cl^-*}_{max}$ were virtually iden-

Table 4. A comparison of the results of the one-substrate kinetic analysis approach and the result of the two-substrate kinetic analysis. See text for further details

	One-substrate analysis	Two-substrate analysis
J_{max} Na^+ (μequiv · kg^{-1} · h^{-1})	420	1642
J_{max} Cl^- (μequiv · kg^{-1} · h^{-1})	286	1696
J_{max} HCO_3^- (μequiv · kg^{-1} · h^{-1})	–	1702
K_m Na^+ (μequiv · l^{-1})	99	–
K_m H^+ (μequiv · l^{-1})	–	0.036 (pH = 7.444)
K_m Cl^- (μequiv · l^{-1})	127	135
K_m HCO_3^- (μequiv · l^{-1})	–	33.3

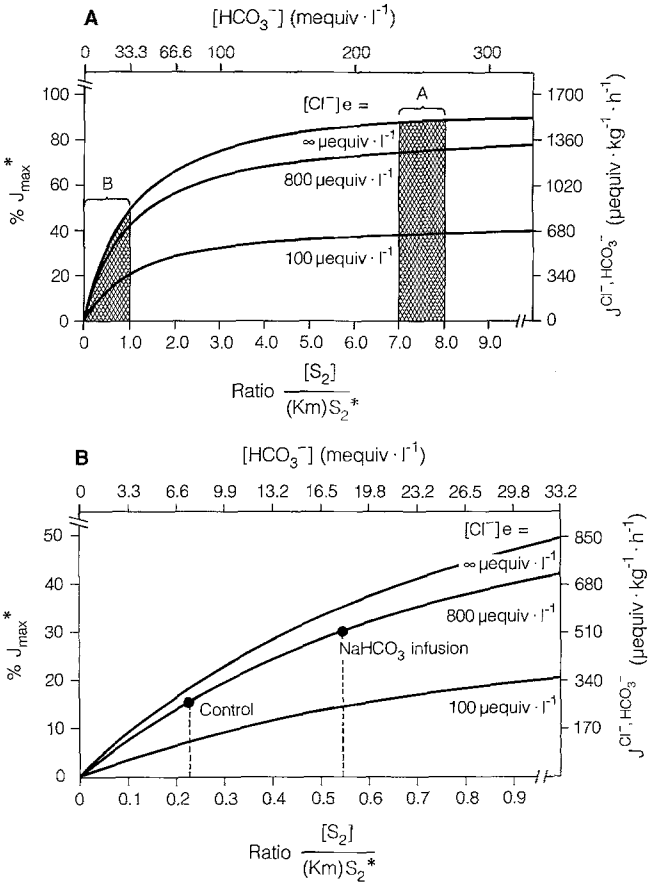

Fig. 6. Theoretical effects of alteration of the $[S_2]/(K_m)S_2^*$ ratio on the rate of transport in a two substrate exchange system, as illustrated by data for the Cl^-/HCO_3^- exchange system in rainbow trout. $(K_m)S_2^*$ was determined by substitution of the appropriate values from Table 4 into the two-substrate equation (Eq. 2). Curves were calculated by varying the internal ion concentration at different external ion (HCO_3^-) concentrations (100, 800, and ∞ μequiv · l^{-1}). Transport rate is expressed as a percentage of J_{max}^* (~1700 μequiv · kg^{-1} · h^{-1}; Table 4). The top and right axis indicate the values of the internal counterion ($[HCO_3^-]$) used and the expected J^{Cl^-,HCO_3^-}. *Region A* indicates where the $[S_2]/(K_m)S_2^*$ is high while *region B* shows the effect of having a low $[S_2]/(K_m)S_2^*$ ratio. Figure 6B is an expanded version of region B in Fig. 6A showing the effects of alteration of $[S_2]/(K_m)S_2^*$ ratios on the rate of transport of the branchial Cl^-/HCO_3^- exchange system. Note that in this figure, the internal counterion concentrations ($[HCO_3^-]$) are physiologically relevant. See text for a detailed explanation

tical (~1700 μequiv · kg^{-1} · h^{-1}) as expected for a 1-for-1 exchange system. Note however, that *true* $J_{max}^{Cl^-,HCO_3^-*}$ was 4–5 times higher (~1700 μequiv · kg^{-1} · h^{-1}) than the *apparent* $J_{max}^{Cl^-}$ (286 μequiv · kg^{-1} · h^{-1}) determined by the one-substrate model under control conditions. Similarly, *true* $J_{max}^{Na^+*}$ (1642 μequiv · kg^{-1} · h^{-1}) was four times higher that the *apparent* $J_{max}^{Na^+}$ (420 μequiv · kg^{-1} · h^{-1}) and very similar to *true* $J_{max}^{Cl^-,HCO_3^-*}$. (*True* $J_{max}^{H^+*}$ and *true* $K_m^{Na^+*}$ could not be determined, as outlined earlier). The high *true* J_{max}^* values for both the Na^+ and Cl^- uptake mechanisms indicates that the fish have very large capacities to take up Na^+ and Cl^- from the water and that normally the transport systems are running at far less than maximal.

The reason for this situation is that *true* $K_m^{H^+*}$ and $K_m^{HCO_3^-*}$ are far higher than the actual $[H^+]$ and $[HCO_3^-]$ in the animal. *True* $K_m^{H^+*}$ is 0.036 μequiv · l^{-1} which corresponds to a pH of 7.444 (Table 4) while control extracellular pH was 7.907 ($[H^+]=0.012$ μequiv · l^{-1}; Table 1). Likewise, *true* $K_m^{HCO_3^-*}$ is 33.3 mequiv · l^{-1} (Table 4) while control extracellular $[HCO_3^-]$ was only 7.10 mequiv · l^{-1} (Table 1). These data result in $[S_2/(K_m)S_2^*$ ratios of 0.34 and 0.21 for the Na^+ and Cl^- transport systems, respectively. The theoretical effect of changing the $[S_2]/(K_m)S_2^*$ ratio on the rate of Cl^-/HCO_3^- transport is illustrated in Fig. 6, based on the two-substrate kinetic constants of Table 4. The *y*-axis represents the rate of transport expressed as a percentage of the true J_{max}^* (1702 μequiv · kg^{-1} · h^{-1}) and the *x*-axis represents the $[S_2]/(K_m)S_2^*$ ratio. The lines yield the calculated transport rates at different $[S_2]/(K_m)S_2^*$ ratios when the external Cl^- concentration is set to fixed values (100 800 and ∞ (100000) μequiv · l^{-1}). $[Cl^-]_e=$ 800 μequiv · l^{-1} represents normal Hamilton tapwater, in which the steady state fluxes of series I (Fig. 1) were performed, 100000 μequiv · l^{-1} represents a saturating concentration, and 100 μequiv · l^{-1} represents a low concentration, slightly below $(K_m)S_1^*$.

The one-substrate model assumes that the concentration of the internal ion is not limiting, i.e., far higher than the measured $(K_m)S_2^*$. In region A, the ratio $[S_2]/(K_m)S_2^*$ is high (7.0–8.0) and therefore the inverse of this ratio $\{(K_m)S_2^*/[S_2]\}$ is very small. The second and third terms in the denominator of Eq. 2 approach zero. Therefore, internal substrate concentration (which at 200–300 mequiv · l^{-1} HCO_3^- is far above the physiological range) has little influence. The relationship between the rate of transport and the external substrate concentration approaches the one-substrate model given in Eqs. 1 and 3.

In region B, the ratio $[S_2]/(K_m)S_2^*$ is very low (<1.0). The second and third terms in the denominator of Eq. 2 become significant, and the rate of transport is then extremely sensitive to the concentration of the internal counterion, which now lies in the physiological range (0–33.3 mequiv · l^{-1} HCO_3^-). For example, in the analysis of the Cl^-/HCO_3^- exchanger, the ratio $[S_2]/(K_m)S_2^*$ was only 0.21 (7.1/33.3) under control conditions. At $[Cl]_e=800$ μequiv · l^{-1}, this yields approximately 15% (252 μequiv · kg^{-1} · h^{-1}) of true $J_{max}^{Cl^-,HCO_3^-*}$ (1702 μequiv · kg^{-1} · h^{-1}), very close to the measured value of 247 μequiv · kg^{-1} · h^{-1} in series I. Increasing the internal $[HCO_3^-]$ from 7.1 mequiv · l^{-1} to 18.2 mequiv · l^{-1} via $NaHCO_3$ infusion increased the $[S_2]/(K_m)S_2$ ratio to 0.54, thereby raising the predicted transport rate to approximately 30% (508 μequiv · kg^{-1} · h^{-1}) of maximal. This was again similar to the measured value (547 μequiv · kg^{-1} · h^{-1}) in series I. The design of the system is such that small changes in internal acid-base status, and therefore counterion concentration, will result in large stimulations or inhibitions of the transport systems. This provides an automatic, negative feedback mechanism for the clearance or retention of acidic and basic equivalents.

Figure 6 also illustrates that the absolute changes in

transport rate effected by a particular change in internal counterion concentration will be greater at higher levels of the external ion. For example, the increase in Cl^-/HCO_3^- transport induced by the rise in $[S_2]/(K_m)S_2^*$ in the preceding example at $[Cl^-]_e = 800$ μequiv · l^{-1} would be about 15% higher at a saturating $[Cl]_e = 100000$ μequiv · l^{-1}, and about 50% lower at $[Cl^-]_e = 100$ μequiv · l^{-1}. This explains the recent report of McDonald et al. (1989) that rates of acid-base adjustment are faster in trout kept in higher $[NaCl]_e$ levels.

The data from the HCl infusion treatment were omitted from the analysis of the Cl^-/HCO_3^- exchanger because the point fell well off the line common to all the other treatments in step 2 (Fig. 4b). According to the two-substrate model, this deviation would indicate a real increase in the number of transporters present in this group. In agreement with this conclusion, morphological analysis of the gills of these fish indicated that there was a large significant increase (about 50%) in chloride cell fractional area due to a proliferation of chloride cell numbers (G.G. Goss, C.M. Wood, S.F. Perry, and P.L. Laurent, unpublished results). The chloride cell is thought to be the site of Cl^- and Na^+ uptake in the freshwater fish gill (Perry and Laurent 1989; Laurent and Perry 1990). Interestingly, the comparable point for Na^+ uptake from the HCl group fell directly on the relationship generated by the other treatments (Fig. 5), despite the marked increase in chloride cells. This suggested that either the chloride cells proliferated without an increase in the number of Na^+ transporters, or that the Na^+ uptake mechanism is not on the chloride cell. Recently, it has been shown in catfish that there is a strong correlation between chloride cell fractional area and Cl^- uptake but that Na^+ uptake and chloride cell fractional area are not correlated. Indeed, in the same study, there was a strong correlation between Na^+ uptake and changes in the morphometry and ultrastructure of the pavement cells (Goss et al. 1991).

Two-substrate versus one-substrate analyses. In conclusion, the two-substrate approach is both experimentally and theoretically more complex than a standard one-substrate Michaelis-Menten analysis. However, the success of this model has important implications for the interpretation of previous and future studies on ion and acid-base regulation in freshwater fish. The analysis demonstrates that the system is counterion-limited; under control conditions, the transporters for Na^+ and Cl^- are working far below their true maximal values. Small changes in internal acid-base status will have large effects on transport rates, providing an automatic negative feedback control for the clearance or retention of acidic or basic equivalents. This influence of internal substrate availability will serve as a rapid, short-term regulatory mechanism until long-term cost-effective mechanisms can be invoked. The latter may involve real changes in the number of transporters present and in the affinity of the transporters for the ions.

The two-substrate model does not discredit the application of one-substrate Michaelis-Menten analysis to situations where there are real changes in the number and/or affinity of transporters [(e.g., chronic adaptation to different salinities; Evans (1984)]. As noted by Kirschner (1988), the use of one-substrate kinetics as a empirical descriptor remains useful *as long as internal acid-base status does not change*. However, the researcher must be aware that changes in acid-base status can alter the *apparent* J_{max} values and the actual rates of ion uptake from the external environment without a change in the number of transporters. A two-substrate analysis is required to test whether changes in ion fluxes result from mechanisms other than internal substrate availability.

Acknowledgements. This study was supported by NSERC Operating and Strategic grants to CMW and a NSERC post-graduate scholarship to GGG. Many thanks to M. Kovacevic and R.S. Munger for excellent technical assistance.

References

Alexander JB, Ingram GA (1980) A comparison of five of the methods commonly used to measure protein concentrations in fish sera. J Fish Biol 16:115–122

Avella M, Bornancin M (1989) A new analysis of ammonia and sodium transport through the gills of the freshwater rainbow trout *(Salmo gairdneri)*. J Exp Biol 142:155–175

Avella M, Masoni A, Bornancin M, Mayer-Gostan N (1987) Gill morphology and sodium influx in the rainbow trout *(Salmo gairdneri)* acclimated to artificial freshwater environments. J Exp Zool 241:159–169

Blaxhall PC, Daisley KW (1973) Routine haematological methods for use with fish blood. J Fish Biol 5:771–781

Boutilier RG, Heming TA, Iwama GK (1984) Physicochemical parameters for use in fish respiratory physiology. In: Hoar WS, Randall DJ (eds) Fish physiology, vol 10A. Academic Press, New York, pp 401–430

Claiborne JB, Heisler N (1984) Acid-base regulation and ion transfers in the carp *(Cyprinus carpio)* during and after exposure to environmental hypercapnia. J Exp Biol 108:25–43

Claiborne JB, Heisler N (1986) Acid-base regulation and ion transfers in the carp *(Cyprinus carpio)*: pH compensation during graded long- and short-term environmental hypercapnia, and the effect of bicarbonate infusion. J Exp Biol 126:41–62

Ehrenfeld J, Garcia-Romeu F, Harvey BJ (1985) Electrogenic active proton pump in *Rana esculenta* skin and its role in ion transport. J Physiol (London) 359:331–355

Evans DH (1984) The role of gill permeability and transport mechanisms in euryhalinity. In: Hoar WS, Randall DJ (eds) Fish physiology, vol 10A. Academic Press, New York, pp 239–283

Florini JR, Vestling CS (1957) Graphical determination of the dissociation constants for two-substrate enzyme systems. Biochim Biophys Acta 25:575–578

Frain WJ (1987) The effect of external sodium and calcium concentrations on sodium fluxes by salt-depleted and non-depleted minnows, *Phoxinus phoxinus* (L.) J Exp Biol 131:417–425

Goss GG, Laurent PL, Perry SF (1991) Evidence for a morphological component in acid-base regulation during environmental hypercapnia in catfish *(Ictalurus nebulosus)*. Cell Tissue Res (in press)

Goss GG, Wood CM (1990a) Na^+ and Cl^- uptake kinetics, diffusive effluxes, and acidic equivalent fluxes across the gills of rainbow trout: I. Responses to environmental hyperoxia. J Exp Biol 152:521–547

Goss GG, Wood CM (1990b) Na^+ and Cl^- uptake kinetics, diffusive effluxes, and acidic equivalent fluxes across the gills of rainbow trout: II. Responses to bicarbonate loading. J Exp Biol 152:549–571

Kirschner LB, Greenwald L, Kerstetter TH (1973) Effect of amiloride on sodium transport across body surfaces of freshwater animals. Am J Physiol 224:832–837

Kirschner LB (1988) Basis for apparent saturation kinetics of Na^+ influx in freshwater hyperregulators. Am J Physiol 254:R984–988

Laurent PL, Perry SF (1990) Effects of cortisol on gill chloride cell morphology and ionic uptake in the freshwater trout, *Salmo gairdneri*. Cell Tissue Res 259:429–442

Maetz J (1972) Branchial sodium exchange and ammonia excretion in the goldfish *Carassius auratus*. J Exp Biol 58:255–275

Maetz J (1973) Na^+/NH_4^+, Na^+/H^+ exchanges, and NH_3 movement across the gills of *Carassius auratus*. J Exp Biol 58:255–275

McDonald DG, Tang Y, Boutilier RG (1989) Regulation of acid and ion transfer across the gills of fish. Can J Zool 67:3046–3054

McDonald DG, Prior ET (1988) Branchial mechanisms of ion and acid-base regulation in the freshwater rainbow trout, *Salmo gairdneri*. Can J Zool 66:2699–2708

McDonald DG, Wood CM (1981) Branchial and renal acid and ion fluxes in the rainbow trout, *Salmo gairdneri*, at low environmental pH. J Exp Biol 93:101–118

Michal G (1985) Determination of Michaelis constant and inhibitor constants. In: Bergmeyer (ed) Methods of enzymatic analysis, vol 1, Verlag Chemie, Weinheim

Milligan CL, Wood CM (1986) Tissue intracellular acid-base status and the fate of lactate after exhaustive exercise in the rainbow trout. J Exp Biol 123:93–121

Perry SF, Laurent PL (1989) Adaptational responses of rainbow trout to lowered external NaCl concentration: contribution of the branchial chloride cell. J Exp Biol 147:147–168

Perry SF, Malone S, Ewing D (1987) Hypercapnic acidosis in the rainbow trout *(Salmo gairdneri)*. I. Branchial ion fluxes and blood acid-base status. Can J Zool 65:888–895

Shaw J (1959) The absorption of sodium ions by the crayfish *Astacus pallipes* (Lereboullet). I. The effect of external and internal sodium concentration. J Exp Biol 36:126–144

Soivio A, Westman K, Nyholm K (1972) Improved method of dorsal aortic catherization: haematological effects followed for three weeks in rainbow trout *(Salmo gairdneri)*. Finn Fish Res 1:11–21

Stetson DL, Steinmetz PR (1983) Role of membrane fusion in CO_2 stimulation of proton secretion by turtle bladder. Am J Physiol 245:C113–C120

Verdouw H, van Echteld CJA, Dekkers, EMJ (1978) Ammonia determinations based on indophenol formation with sodium salicylate. Water Res 12:399–402

Wood CM (1988) Acid-base and ionic exchanges at gills and kidney after exhaustive exercise in the rainbow trout. J Exp Biol 136:461–481

Wood CM, Jackson EB (1980) Blood acid-base regulation during environmental hyperoxia in the rainbow trout *(Salmo gairdneri)*. Respir Physiol 42:351–372

Wood CM, Randall DJ (1973) Sodium balance in the rainbow trout *(Salmo gairdneri)* during extended exercise. J Comp Physiol 82:235–256

Wood CM, Wheatly M, Höbe H (1984) The mechanisms of acid-base and ionoregulation in the freshwater rainbow trout during environmental hyperoxia and subsequent normoxia. III. Branchial exchanges. Respir Physiol 55:175–192

Wright PA, Randall DJ, Wood CM (1988) The distribution of ammonia and H^+ between tissue compartments in lemon sole *(Parphrys vetulus)* at rest, during hypercapnia, and following exercise. J Exp Biol 136:149–175

Wright PA, Wood CM (1985) An analysis of branchial ammonia excretion in the freshwater rainbow trout: effects of environmental pH change and sodium uptake blockade. J Exp Biol 114:329–353

Zall DM, Fisher MD, Garner QM (1956) Photometric determination of chlorides in water. Anal Chem 28:1665–1678

Zeidler R, Kim HD (1977) Preferential haemolysis of postnatal calf red cells induced by internal alkalinization. J Gen Physiol 70:385–401